ELSEVIER

Neurobiology of Disease

www.elsevier.com/locate/ynbdi
Neurobiology of Disease 24 (2006) 245–253

A K_v4.2 truncation mutation in a patient with temporal lobe epilepsy

Baljinder Singh,[a,1] Ikuo Ogiwara,[a,1] Makoto Kaneda,[b] Natsuko Tokonami,[a] Emi Mazaki,[a] Koichi Baba,[c] Kazumi Matsuda,[c] Yushi Inoue,[c] and Kazuhiro Yamakawa[a,*]

[a]*Laboratory for Neurogenetics, RIKEN Brain Science Institute, Saitama 351-0198, Japan*
[b]*Department of Physiology, Keio University School of Medicine, Tokyo 160-8582, Japan*
[c]*National Epilepsy Center, Shizuoka Institute of Epilepsy and Neurological Disorders, Shizuoka 420-8688, Japan*

Received 6 March 2006; revised 12 June 2006; accepted 5 July 2006
Available online 24 August 2006

Temporal lobe epilepsy (TLE) has a multifactorial etiology involving developmental, environmental, and genetic components. Here, we report a voltage-gated potassium channel gene mutation found in a TLE patient, namely a K_v4.2 truncation mutation. K_v4.2 channels, encoded by the *KCND2* gene, mediate A currents in the brain. The identified mutation corresponds to an N587fsX1 amino acid change, predicted to produce a truncated K_v4.2 protein lacking the last 44 amino acids in the carboxyl terminal. Electrophysiological analysis indicates attenuated K^+ current density in cells expressing this K_v4.2-N587fsX1 mutant channel, which is consistent with a model of aberrant neuronal excitability characteristic of TLE. Our observations, together with other lines of evidence, raise the intriguing possibility of a role for *KCND2* in the etiology of TLE.

Keywords: Temporal lobe epilepsy; *KCND2*; K_v4.2; Potassium channel; Truncation mutation; A currents

Introduction

In temporal lobe epilepsy (TLE), arguably the most common epilepsy syndrome, pharmacoresistant cases are frequently encountered. Complete seizure control in such refractory patients often requires invasive surgical therapies. TLE has historically been viewed as an acquired syndrome, but there is an emerging consensus that some TLEs have genetic components (Engel, 2001; Vadlamudi et al., 2003). For example, mutations in *LGI1* cause autosomal dominant partial epilepsy with auditory features (Kalachikov et al., 2002), a rare monogenic type of TLE. Nonetheless, elucidation of pathogenesis in the more common, polygenic TLEs remains elusive.

There has been a steady accumulation of findings and observations linking K_v4.2, a primary pore-forming (α) subunit member within the Shal subfamily of voltage-gated potassium channels, with epilepsies including TLE. Within the brain, K_v4.2 mediates A currents (I_A), which play crucial roles in the regulation of back-propagating action potentials (bAPs) in neuronal dendrites (Hoffman et al., 1997). Hence, disruptions in these physiologically important I_A could lead to dysregulation of neuronal excitability, a hallmark of epilepsy. Indeed, convulsive activity can be induced in rats and mice by the use of selective pharmacological blockers of I_A (Bagetta et al., 1992; Juhng et al., 1999).

Reports in animal epileptic models have also correlated changes in I_A and reductions in K_v4.2 expression with increased seizure activity (Tsaur et al., 1992; Birnbaum et al., 2004). In the methylazoxymethanol rat model of cortical dysplasia and epilepsy, a dramatic reduction in K_v4.2 expression is observed in hyperexcitable heterotopic neurons (Castro et al., 2001). Observations specifically linking changes in K_v4.2 activity with hippocampal dendritic excitability were recently reported in pilocarpine-treated rats, a pathophysiological model of human TLE (Bernard et al., 2004). These authors found that epileptic rats demonstrated more active and sustained bAPs in the soma and dendrites of hippocampal neurons than did control animals following pilocarpine treatment, which triggers prolonged seizures in this model (Bernard et al., 2004). They proposed that in TLE, I_A-mediated control of bAP amplitude may be compromised due to lowered availability of K_v4.2 channels at critical dendritic locations, which in turn contributes to the positive feedback loops underlying epileptic seizures. Finally, also germane to this thesis, K_v4.2 null mice have an increased susceptibility to kainate-induced seizures (Barnwell et al., 2004).

Comparatively less information is available on I_A changes in human epilepsy. In a study on voltage and Ca^{2+}-dependent K^+ currents in dentate granule cells acutely isolated from resected hippocampi of patients with refractory TLE, a marked down-regulation of classical I_A was observed in cells from patients with lesion-associated TLE (Beck et al., 1997). I_A exhibiting possible disease-related variations in steady-state inactivation properties—with specific pharmacosensitivities suggesting mediation by K_v1.4 or K_v4 family α-subunits—were described in acutely isolated temporal lobe neurons from epilepsy patients with complex partial seizures (Rüschenschmidt et al., 2004).

* Corresponding author. Fax: +81 48 467 7095.
E-mail address: yamakawa@brain.riken.jp (K. Yamakawa).
[1] These authors contributed equally to this study.
Available online on ScienceDirect (www.sciencedirect.com).

0969-9961/$ - see front matter © 2006 Elsevier Inc. All rights reserved.
doi:10.1016/j.nbd.2006.07.001

A corollary of these observations is that mutations in *KCND2* may occur in human TLE. We report here a potassium channel gene mutation in a TLE patient—a *KCND2* 5-bp deletion leading to a channel protein with a carboxyl terminal truncation and altered electrophysiological properties.

Materials and methods

TLE patients

We recruited 69 unrelated, TLE-diagnosed individuals of Japanese descent for this study. All 69 TLE patients fulfilled established clinical criteria for the disease and were diagnosed and treated at the National Epilepsy Center, Shizuoka Institute of Epilepsy and Neurological Disorders, Shizuoka, Japan. Each adult participant or where necessary, responsible guardians of adult subjects, as well as the parents and/or legal guardians of subjects who were minors at the time the study began signed an informed consent form as approved by the Ethics Committee at the National Epilepsy Center. The entire study was approved by the Ethics Committees in both the National Epilepsy Center and the RIKEN Brain Science Institute.

The 31-year-old female proband harboring the c.2723_2727delAAACT mutation (K_v4.2-N587fsX1; see Table 1) is the only member of her family with epilepsy. The first notable manifestation of her epilepsy, at age 13, involved a convulsive seizure with head version and facial retraction towards the right. At this point, she was started on valproate therapy. Three months later, she began to have complex partial seizures with oral automatisms lasting for 1–2 min. There was no aura. She experienced such seizures three times a month, but after adding carbamazepine, she was seizure-free for 18 months. However, at age 16, the seizures recurred and repeated 2–10 times a month in spite of her receiving various medications.

Table 1
KCND2 mutation and SNPs in Japanese TLE patients

No	Disease mutation	Frequency
1	c.2723_2727delAAACT(N587fsX1)	1/69 TLE patients; 0/112 normal controls
No	**Coding SNP**	**Frequency**
1	c.756 C>T (C252C)	1/69 TLE patients; 1/112 normal controls
No	**Non-coding SNP**	**Frequency**
1	IVS3+40T>C	2/69 TLE patients; 0/112 normal controls
2	IVS3+68T>C	1/69 TLE patients; 6/112 normal controls

Four different nucleotide changes were identified in our pool of 69 Japanese TLE patients. Two nucleotide changes were found only in patients and not in normal, healthy control individuals: a heterozygous 5-bp nucleotide deletion, c.2723_2727delAAACT, and a heterozygous non-coding region SNP, IVS3+40T>C. The heterozygous coding region silent mutation, c.756 C>T (C252C), was found in only one patient and also in 1 of 112 unrelated, healthy individuals. One other heterozygous non-coding region SNP, IVS3+68T>C, was found in 1 TLE patient and also in 6 of 112 unrelated, healthy individuals.

Our group first examined her when she visited the National Epilepsy Center at age 25 years. Her seizures were found to consist of swinging of the body followed by motionless staring and oral automatisms. In visual object processing task tests, she could name objects 2 min after seizures. The EEG showed spikes and sharp waves mostly in the left anterior temporal region, although they were rarely observed to occur independently in the right side. Standard EEG analysis showed ictal discharge spreading from the left anterior temporal region to the right side 15 s after the discharge onset. The behavior onset preceded the EEG discharges. Although these and other functional studies using magnetoencephalography methods implicated the left temporal region in epileptogenesis, neuroimaging data from MRI and interictal SPECT were unremarkable. An invasive, intracranial EEG evaluation was therefore used to map the left mesio-basal temporal region as the source of the anomalous discharge activity, with 11 recorded seizures beginning in this area (see Fig. 2). The interictal discharges were more prominent in the basal temporal area than in the medial temporal area. Evaluations of her cognitive functions were determined using the Wechsler Adult Intelligence Scale-R in which she scored 59 and the Wechsler Memory Scale-R memory quotient, for which her score was 64.

To extirpate the epileptogenic tissue, a first attempt was performed at age 27 years, via selective left amygdalo-hippocampectomy, in which the amygdala and hippocampus were resected while the lateral temporal neocortex was untouched. Unfortunately, intractable seizures recurred 6 months post-surgery, necessitating a second, more extensive surgical intervention, *viz.* left anterior temporal lobectomy, to finally abolish ictal activity. She has now remained free from seizures for more than 3 years. There was no evidence of medial temporal sclerosis or any other overt pathology within the resected specimens.

Mutational analysis of KCND2

We screened the 69 TLE patients for mutations in *KCND2* by directly sequencing all six coding and boundary regions. Genomic DNA was extracted from heparin-treated blood samples using the QIAamp DNA Blood Mini Kit (Qiagen, Hilden, Germany) and from hair and buccal samples using the ISOHAIR Kit (Nippon Gene, Toyama, Japan). All genomic DNA samples were first amplified by PCR, and the PCR products were analyzed by direct sequencing utilizing the ABI 3700 capillary automated-sequencing system (PE Applied Biosystems, Foster City, CA). To characterize heterozygous mutations, specific PCR products were also subcloned into pCR-Blunt II-TOPO (Invitrogen, Carlsbad, CA) and multiple independent subclones were sequenced. For PCR reactions, the Pwo (Roche Molecular Biochemicals, Mannheim, Germany), Pyrobest (Takara, Tokyo, Japan), and Blend Taq Plus (Toyobo, Tokyo, Japan) DNA Polymerase systems were used according to manufacturer's instructions. Primer sequences are available upon request.

Construction of wild-type and mutant KCND2 expression vectors

cDNA for wild-type human *KCND2* was synthesized from normal human total brain poly (A) RNA (Clontech, Palo Alto, CA) using SuperScript III Reverse Transcriptase (Invitrogen). The resulting cDNAs were subsequently amplified by PCR using a 5′ oligonucleotide primer containing a *Bgl*II site and a 3′ primer containing an *Eco*RI site. The resulting amplicons were first

inserted into pCR-Blunt II-TOPO (Invitrogen) and then subcloned between the *Bgl*II and *Eco*RI sites of pIRES2-EGFP (Clontech). The mutant vector was generated from the wild-type vector using the QuikChange Site-Directed Mutagenesis kit (Stratagene, La Jolla, CA). All constructs were verified by sequencing.

Cell culture and transfection

HEK293 cells were grown in Dulbecco's modified Eagle's medium supplemented with 10% (v/v) heat-inactivated fetal bovine serum, penicillin (100 U/mL) and streptomycin (100 mg/mL) and maintained at 37°C in a humidified 5% CO_2 incubator. For whole-cell patch-clamping, HEK293 cells were first plated on poly-lysine-coated 6-well dishes and then transfected, the next day, with 1 μg of pKCND2-IRES2-EGFP or pKCND2 (N587fsX1)-IRES2-EGFP, or 500 ng of pKCND2-IRES2-EGFP and 500 ng of pKCND2 (N587fsX1)-IRES2-EGFP using Fugene6 (Roche Molecular Biochemicals) according to the manufacturer's instructions. For patch-clamp analysis, HEK293 cells were plated on poly-lysine-coated coverslips (Sumitomo Bakelite Co., Tokyo, Japan) 24 h after transfection.

For cell surface expression assays, HEK293 cells were transfected with 2.5 μg of pKCND2-IRES2-EGFP or pKCND2 (N587fsX1)-IRES2-EGFP together with 2.5 μg of a control plasmid, pcDNA3.1(+)CD8/Myc-His A, using Lipofectamine 2000 (Invitrogen) according to the manufacturer's instructions.

Cell surface expression assay

We used the cell surface protein biotinylation and purification kit (Pierce Biotechnology, Rockford, IL) to isolate $K_v4.2$ WT and mutant proteins expressed on the HEK293 cell surface. HEK293 cells were first washed three times with PBS/Ca^{2+}/Mg^{2+} (10 mM phosphate buffer, 2.7 mM KCl, 137 mM NaCl, 2.5 mM $CaCl_2$, and 1 mM $MgCl_2$, pH 7.4), incubated with 1 mg/mL of EZ-link Sulfo-NHS-SS-Biotin (Pierce Biotechnology) in PBS/Ca^{2+}/Mg^{2+} for 30 min at 4°C, and then washed three times with 100 mM glycine in PBS/Ca^{2+}/Mg^{2+}. Total lysates were prepared by washing the cells twice with PBS/Ca^{2+}/Mg^{2+} and suspending the scraped cells in precipitation buffer (PB; 0.1% SDS, 0.5% sodium deoxycholate, 1% NP-40, and 1× complete protease inhibitor cocktail (Roche Molecular Biochemicals) in PBS), which were sonicated and then centrifuged for 10 min at 15,000 rpm. The supernatants were incubated with 50 μL of immobilized NeutrAvidin gel (Pierce Biotechnology) for 1 h at room temperature (RT) using a rotator, after which the gel was washed five times with wash buffer (Pierce Biotechnology). The biotinylated proteins were first eluted by adding 20 μL of 2 M Urea, 50 mM DTT, 1× NuPAGE reducing agent (Invitrogen), and 1× NuPAGE LDS sample buffer (Invitrogen) into the gel and incubating this mixture for 1 h at RT. Eluted proteins were then incubated for 10 min at 70°C, separated on the NuPAGE Novex Tris–acetate 3–8% gel (Invitrogen), transferred to a nitrocellulose membrane (Schleicher and Schuell, Dassel, Germany), and immunoblotted. Blots were probed with a rabbit polyclonal antibody against the N-terminus of $K_v4.2$ (Alomone Labs, Jerusalem, Israel) or a rabbit monoclonal antibody against an Myc epitope tag (Cell Signaling Technology, Beverly, MA). The blot was then incubated with horseradish-peroxidase (HRP)-conjugated secondary antibody (Santa Cruz Biotechnology, Santa Cruz, CA), and bound antibodies were detected using enhanced chemiluminescence reagent (PerkinElmer Life Sciences, Boston, MA). A total of three separate experiments were completed.

For protein dot blot assays, the biotinylated proteins were purified with the NeutrAvidin gel and spotted directly on a membrane. Biotinylated $K_v4.2$ proteins were immunodetected as described above. Quantification was performed using the LAS-1000 luminescent image analyzer (Fuji Photo Film, Tokyo, Japan). A total of two independent assays were performed.

Patch-clamp analysis

Data recordings

Using an inverted microscope (IX70, Olympus, Tokyo, Japan), GFP-positive transfected HEK293 cells were selected for electrical recordings. To minimize space-clamp problems, GFP-positive cells in syncytia were not considered and only strongly fluorescent cells were selected. The external solution was adjusted to pH 7.4 with NaOH and contained (in mM): NaCl, 135; KCl, 4.0; $CaCl_2$, 1.0; $MgCl_2$, 2.0; glucose, 10; and HEPES, 10. Pipette electrodes were made from borosilicate glass capillary tubes (0.8–1.0 mm inner diameter, Hilgenberg GmbH, Marsfeld, Germany) using a multi-step horizontal puller (P-97, Sutter Instrument Co., Novato, CA). The pipette solution was pH adjusted to 7.2 with KOH and was composed of (in mM): KCl, 135; $MgCl_2$, 1.0; EGTA, 10; glucose, 5.0; and HEPES, 10. Pipette resistance was 1.0–3.5 MΩ when filled with internal pipette solution. Except for the very tip, the outer wall of the pipette was coated with dental wax to reduce stray capacitance (GC Corporation, Tokyo, Japan). The reference electrode was an Ag–AgCl pellet in a well that was connected to the bath using a 150 mM NaCl-filled agar bridge. Currents were recorded using an Axopatch 200B amplifier (Axon Instruments, Burlingame, CA). Current and voltage signals were filtered using a low-pass Bessel filter with a cut-off frequency at 10 kHz and stored on a hard disk in V450JS2 (Iiyama, Nagano, Japan); "pclamp 8.0" software was used throughout (Axon Instruments, Burlingame, CA). The values in all pulse protocols were programmed on the computer. Cell capacitances were calculated using "pclamp 8.0" software. Capacitative currents and series resistances were electronically compensated. All experiments were carried out at RT (22°C). The electrophysiologist performing all experimental recordings was blinded to the HEK293 cell genotypes used.

Data analysis

For current density comparisons, peak amplitudes of K^+ current were normalized relative to total cell capacitance. For conductance–voltage relationship comparisons, K^+ currents were evoked by 400 ms depolarizations to various test potentials (−70 mV to 70 mV) from a holding potential of −80 mV. Since step depolarization only produced an ohmic conductance below −60 mV under our experimental conditions, leak currents at individual potentials were estimated using a linear regression line fit to the −80, −70, and −60 mV data points. Current–voltage relationships were constructed after subtraction of leak currents. Potassium conductance (g_k) was calculated according to the equation, $g_k = I_K/(V_g - E_r)$, where I_K is the peak amplitude of the K^+ current, V_g is the test potential, and E_r is the reversal potential for K^+. In the present study, E_r was calculated by the Nernst equation, $E_r = 58\log(\gamma_o[K^+]_o/\gamma_i[K^+]_i)$, where γ_o and γ_i are the activity coefficients of the extra- and intracellular K^+ respectively, and $[K^+]_o$ and $[K^+]_i$ are the extra- and intracellular K^+ concentrations respectively. In the present study, $[K^+]_o$ was

155 mM (including the concentration of KOH), $[K^+]_i$ was 4 mM, γ_o was 0.75, and γ_i was 0.94. Using these parameters, E_r was assumed to be −86 mV. Potassium conductances recorded at individual test potentials were normalized to the conductance recorded at 70 mV.

To compare steady-state voltage dependence of inactivation, cells were prepulsed for 2 s at various holding potentials (from −120 mV to 10 mV in 10 mV increments), and K^+ currents were then evoked by a step depolarization to 0 mV. The peak amplitudes of the K^+ currents measured at individual test potentials were normalized to the peak amplitude of the K^+ current measured at a holding potential of −80 mV. Data points were fitted by the least-squares fit of the data to a Boltzmann function, according to the equation $I/I_{max}=1/\{1+\exp[(V_h-V_{1/2})/k]\}$, where I_{max} is the magnitude of the peak K^+ current observed at a holding potential of −120 mV, V_h is the holding potential, $V_{1/2}$ is the potential at which the K^+ current is one-half maximal and k is the slope factor. In the double pulse protocol, two depolarizing pulses (step to 10 mV, 200 ms in duration) with various interpulse interval (from 0.1 s to 5 s) were successively applied to activate K^+ currents. The peak amplitude of K^+ currents evoked by the second pulse (I) was normalized to the peak amplitude of K^+ currents evoked by the first pulse (I_{max}) and I/I_{max} is expressed as recovery ratios.

Results

Mutational analysis of KCND2 in TLE patients

We screened 69 unrelated, TLE-diagnosed individuals of Japanese descent for mutations in the *KCND2* gene by directly sequencing all six coding regions and their exon–intron boundary regions.

A total of four different nucleotide changes were identified in our pool of 69 Japanese TLE patients (Table 1). One of these, a heterozygous 5-bp nucleotide deletion, c.2723_2727delAAACT, causes a frame-shift that introduces a premature stop codon at Asn587 immediately after the shift (N587fsX1) (Fig. 1). This finding takes on added significance when viewed in the context of the NCBI SNP database, which lists only one coding region change, a silent mutation, out of an aggregate of almost 1000 SNPs for the *KCND2* gene. This mutant channel protein, which we have designated K_v4.2-N587fsX1, is predicted to lack the last 44 carboxyl-terminal amino acids (Figs. 1B, D). This deleted region harbors three critical ERK phosphorylation sites (aa. T602, T607, S616; Adams et al., 2000; Yuan et al., 2002) and interacting motifs for the cytoskeletal proteins PSD-95 (aa. 627–630 [VSAL]; Wong et al., 2002) and filamin (aa. 601–604 [PTPP]; Petrecca et al., 2000).

The proband with this mutation was diagnosed with TLE, although no detectable histological abnormalities were found. She also displayed cognitive impairment preceding her history of epilepsy. Beginning at age 13, she has had a complicated history of medically refractory seizures, which ranged from complex partial with motionless staring and oral automatisms to convulsions. The epilepsy was prominently pharmacoresistant as very limited seizure control was observed with any available antiepileptic medications. An invasive, intracranial EEG evaluation mapped the left mesio-basal temporal region as the source of the anomalous discharge activity (Fig. 2). In fact, 11 recorded seizures all began in the left mesio-basal temporal area. The interictal discharges were more prominent in the basal temporal area than in the medial temporal area. Complete cessation of seizures was only achieved at age 28,

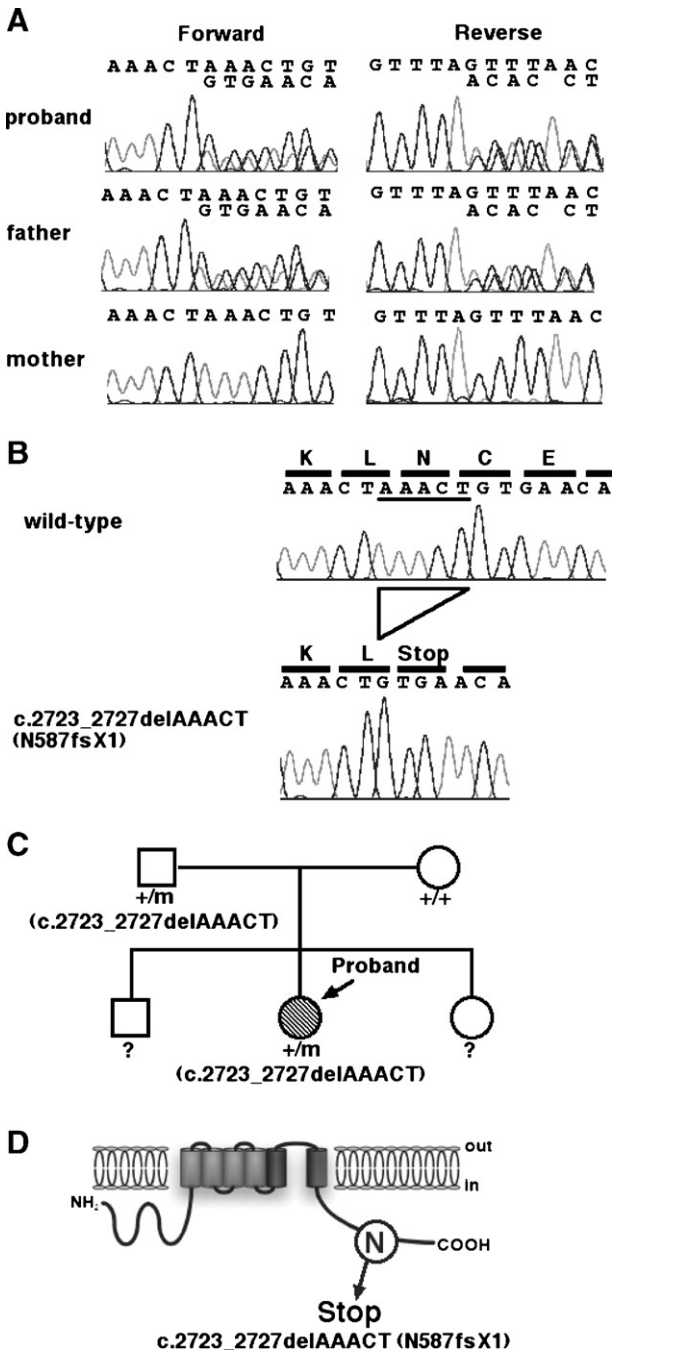

Fig. 1. A heterozygous 5-bp deletion in *KCND2* results in a truncated K_v4.2 channel protein in a TLE patient. (A) Electropherograms obtained by direct sequencing of purified *KCND2* exon 6 genomic DNA PCR products show superimposition of normal and mutant alleles downstream of a mutation. The heterozygous mutation is found in genomic DNA samples from both the proband and the father but not from the mother. Both forward and reverse sequencing reactions were analyzed. (B) Electropherograms of mutant and wild-type alleles from both the proband and her father. The mutation, a 5-bp deletion, c.2723_2727delAAACT, creates a frame-shift resulting in a premature stop codon (TGA) at Asn587 (N587fsX1). (C) The c.2723_2727delAAACT mutation was identified in a proband with TLE, and in her asymptomatic father, whereas the *KCND2* gene was normal in the asymptomatic mother. We did not have access to genomic DNA from the 2 asymptomatic siblings. (D) The premature stop codon at Asn587 (N587fsX1) results in a truncated K_v4.2 protein lacking aa. 587–630.

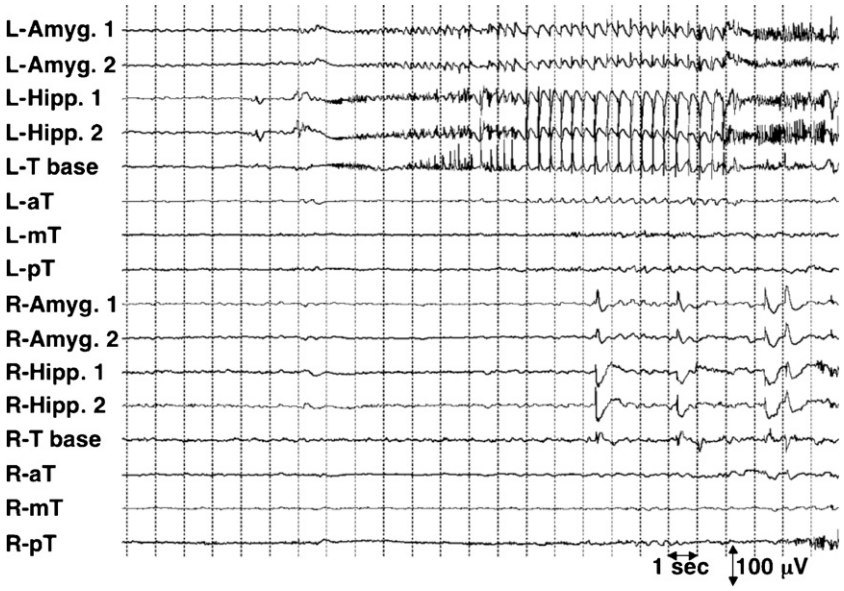

Fig. 2. An ictal intracranial EEG recording from the proband. The ictal discharge started at the mesio-basal temporal area including temporal base, hippocampus, and amygdala on the left side. The discharge then spread to the whole temporal lobe bilaterally (L, left; R, right; Amyg., amygdala; Hipp., hippocampus; T base, temporal base; aT, anterior temporal lateral cortex; mT, middle temporal lateral cortex; pT, posterior temporal lateral cortex).

after two surgical interventions in quick succession (see Materials and methods for more of the proband's clinical details).

Genomic DNA from lymphocytes from the asymptomatic proband's father also harbored the heterozygous K_v4.2-N587fsX1 mutation (Figs. 1A, C), as did genomic DNAs from the father's hair and buccal swab samples. The mutant and wild-type alleles from both the proband and her father were analyzed separately by direct sequencing of PCR products subcloned into pCR-Blunt II-TOPO. Twenty clones each were analyzed for both the proband and father.

This mutation was not found in a pool of 224 chromosomes obtained from unrelated, healthy control individuals. DNAs from the proband's asymptomatic elder brother and sister, as well as those from her grandparents, were not available for the study (Fig. 1C).

The heterozygous non-coding region SNP, IVS3+40T>C, was found in 2 TLE patients but was absent in a pool of 224 chromosomes obtained from unrelated, healthy individuals (Table 1). The heterozygous coding region silent mutation, c.756 C>T (C252C), was found in only one TLE patient and also in 1 unrelated, healthy individual. Both c.756 C>T (C252C) and IVS3+40T>C are not listed in either the NCBI or Japanese SNP databases. One other heterozygous non-coding region SNP, IVS3+68T>C, is listed in the NCBI database as NCBI refSNP ID: rs7795370.

Truncated K_v4.2 channels lead to decreased K^+ current density

Using whole-cell patch-clamp recordings, we analyzed the electrophysiological properties of the human K_v4.2 wild-type and K_v4.2-N587fsX1 mutant channels expressed in HEK293 cells.

Recordings were initiated when the holding current was <200 pA after adopting the whole-cell configuration; this routinely required 5 min of intracellular perfusion. Fig. 3A shows the transient K^+ currents elicited by a depolarizing voltage step (from −70 to 70 mV), from a holding potential of −80 mV, in cells with WT K_v4.2 channels. The transient K^+ current reached a peak within 25 ms and inactivated gradually. The extrinsic origin of the transient K^+ currents was confirmed by the absence of transient K^+ current in non-transfected HEK 293 cells. In cells expressing the K_v4.2-N587fsX1 mutant channel, transient K^+ current amplitudes tended to be smaller than those for cells harboring WT K_v4.2 channels (data not shown) even though the surface expression levels of mutant channels were similar to wild-type channel levels (see the following section and Fig. 4). To exclude potential problems introduced by cell size variations, we calculated the current density per unit membrane using the capacitance of recorded cells since the capacitance per unit membrane has a uniform value. Current density exhibited by cells with the K_v4.2 mutant channels (n=11) was significantly lower than that in cells harboring wild-type channels (n=20) (Fig. 3B). In cells expressing both wild-type and mutant channels (n=14), current density was not significantly different from that in cells with wild-type channels alone, although it only reached a level intermediate between values recorded in cells with either wild-type or mutant channels (Fig. 3B). To rule out any possible variation in channel expression levels among HEK293 cells, we reduced the amount of transfected cDNA from 1 μg to 500 ng and repeated the same experiments. We confirmed that the current density reduction observed earlier in cells harboring mutant channels was also evident in this series of experiments (data not shown; number of cells examined were 10 for wild-type, 8 for wild-type and mutant together, and 10 for mutant).

Next, we investigated the conductance–voltage relationship. K_v4.2 channel conductance increased sigmoidally as the potential of the prepulse was stepped toward more positive potentials (Fig. 3C). Half activation potentials were −9.4±7.4 mV (n=20) for WT, −7.3±9.9 mV (n=14) for the WT+K_v4.2-N587fsX1, and −4.9±11.3 mV (n=11) for the K_v4.2-N587fsX1 mutant channel and were not significantly different among any of the three cell groups (p>0.05). Steady-state inactivation increased sigmoidally as the potential of the prepulse was stepped toward more positive potentials (Fig. 3D). Half inactivation potentials

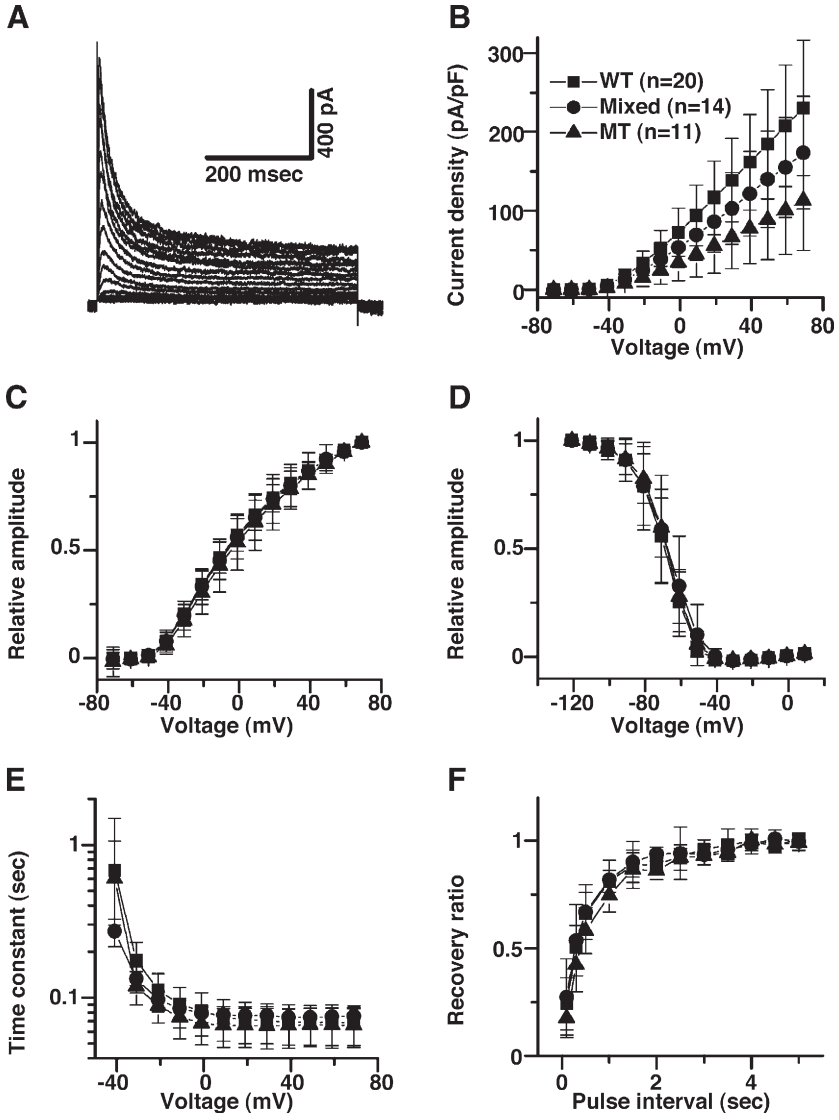

Fig. 3. Decreased K^+ current density in K_v4.2-N587fsX1 channels. Voltage-gated potassium currents recorded from HEK293 cells expressing wild-type human K_v4.2 channels only, wild-type and mutant K_v4.2-N587fsX1 channels together, and mutant K_v4.2-N587fsX1 channels only. (A) Voltage-gated transient potassium currents of wild-type channels. Currents were evoked by a step depolarization (from −70 mV to 70 mV, pulse interval 15 s) from a holding potential of −80 mV. (B–F): symbols: wild-type (WT, closed squares), wild-type+ mutant (Mixed, closed circles), and mutant (MT, closed triangles); each point represents mean±SEM. (B) Current density–voltage relationship of K^+ currents in HEK 293 cells. Cells expressing only mutant K_v4.2-N587fsX1 proteins show significantly lower current density compared to cells with wild-type channels ($p<0.001$, −30 mV or more positive potentials). The data points represent the average current density of the pooled data. Number of cells examined WT: 20, Mixed: 14, MT: 11. (C) Conductance–voltage relationship. The data points represent the average of the pooled data. There were no significant differences among the three groups. (D) Steady-state voltage dependence of inactivation. The data points represent the average of the pooled data. There were no significant differences among the three groups. (E) Time constant of inactivation of the voltage-gated transient K^+ current. Inactivation phase of transient K^+ current was curve fitted by the single exponential function. The data points represent the average of the pooled data (number of cells, WT: 9, Mixed: 5, MT: 8). There were no significant differences among the three groups. (F) Speed of recovery from inactivated state. The data points represent the average of the pooled data. There were no significant differences among the three groups.

were −70.1±7.1 mV ($n=13$) for WT, −67.8±9.2 mV ($n=17$) for the WT+K_v4.2-N587fsX1, and −68.2±5.1 mV ($n=12$) for the K_v4.2-N587fsX1 mutant channel and were not significantly different among any of the three cell groups ($p>0.05$).

To assess the time constant of inactivation of transient K^+ currents, we curve fitted the inactivation phase of transient K^+ currents with single exponential functions (Fig. 3E). There were no significant differences in the time constants among the three groups.

To examine any effects on the recovery from inactivation, we compared the recovery times from the inactivated state by using a double pulse protocol. We defined recovery speeds as the interpulse intervals at which the K^+ currents retrieved 63% of the control value. Recovery speeds were 0.56±0.2 s for WT ($n=9$), 0.54±0.29 s for the WT+K_v4.2-N587fsX1 ($n=8$), and 0.73±0.22 s for the K_v4.2-N587fsX1 mutant channel ($n=6$) (Fig. 3F). Recovery times were not significantly different among the three sample groups ($p>0.05$).

To examine whether the observed current density reductions in cells harboring the K_v4.2-N587fsX1 mutant channels were due to channel conductance reductions, we tried to record single channels

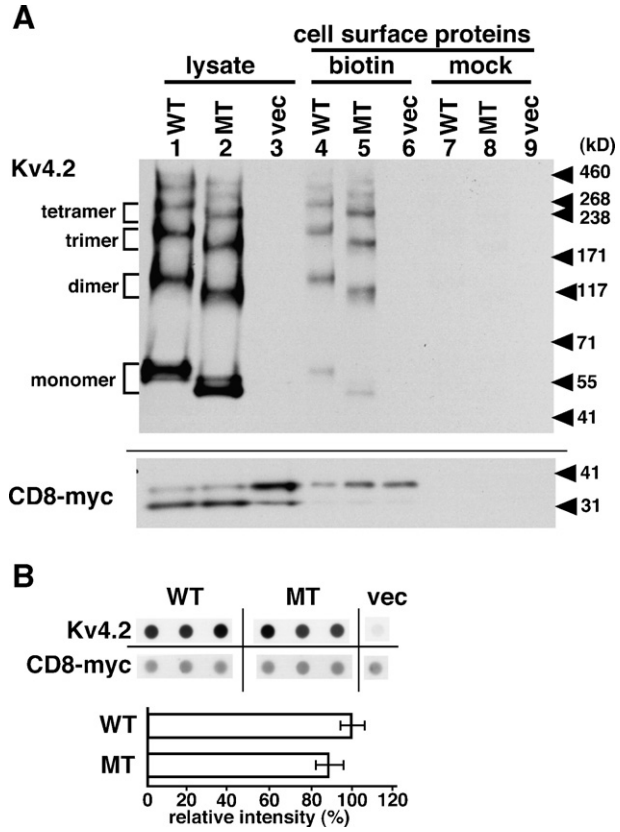

Fig. 4. Wild-type and mutant K_v4.2-N587fsX1 channels have similar total cell surface expression levels in HEK cells. Both recombinant wild-type and mutant K_v4.2-N587fsX1 channels are expressed on the surface of transiently transfected HEK293 cells. (A) For total cell expression (lanes 1–3), HEK293 cells expressing wild-type or mutant K_v4.2-N587fsX1 channels were lysed, the proteins separated by PAGE, and electroblotted onto nitrocellulose filters. Filters were incubated with an anti-N-terminus K_v4.2 antibody and antibody reactive bands were detected with enhanced chemiluminescence reagent. For cell surface expression (lanes 4–9), cells were first incubated either with or without NHS-SS-Biotin and then lysed. The biotinylated or mock-treated cell-surface proteins were then precipitated with avidin gel and analyzed by Western blotting as above. Relative transfection efficiencies were checked using CD8 protein (with C-terminal myc and His fusion tags) co-expression levels displayed in the blot below. The blots shown here are representative of our collective findings since the results from three independent experiments were concordant. (B) Protein dot blot assays were performed using an anti-N-terminus K_v4.2 antibody. The lower panel shows mean signal intensity for biotinylated mutant proteins represented as a percentage relative to that for biotinylated wild-type proteins (100%) and demonstrates that there were no significant differences in surface protein expression levels ($p>0.05$). Error bars represent SEM (wild-type: $n=3$; mutant: $n=3$).

in both the cell attached mode and outside-out recording mode. However, we could not record any channel activity in the cell attached mode whereas outside-out mode recording results were not obtained consistently enough to allow for statistical analysis.

K_v4.2-N587fsX1 channel surface expression levels are unaffected in HEK cells

In order to investigate whether the cell surface expression of mutant channel proteins may be affected in neurons, we expressed the K_v4.2-N587fsX1 protein in HEK293 cells, and biotinylated total surface-expressed proteins, which were then purified and analyzed in Western blots (Fig. 4A). As seen in the lanes marked 'lysate' (Fig. 4A, lanes 1 and 2), total cellular K_v4.2-N587fsX1 mutant protein expression did not differ markedly from WT channel expression. Furthermore, the results of the cell surface protein biotinylation assays indicate that surface expression levels of WT and K_v4.2-N587fsX1 proteins did not differ significantly (Fig. 4A, lanes 4 and 5). The 630 amino acid WT K_v4.2 protein has a predicted mass of 70.5 kDa calculated by the UniProtKB/Swiss-Prot database, and tetramers should be about 282 kDa in size. The computed molecular weight of the K_v4.2-N587fsX1 mutant protein is approximately 66 kDa (determined using the 'Compute pI/Mw' tool on "ABI's Bioinformatics Toolkit" website) with tetramers of about 264 kDa in mass. It is not clear why, under the gel running conditions used, apparently stable oligomeric forms of both WT and K_v4.2-N587fsX1 proteins were observed. Biotinylated proteins corresponding to tetramers were clearly visible among these 'stable oligomers' for both mutant (264 kDa) and WT (282 kDa) channels (Fig. 4) This is not unexpected since the primary subunits of all K^+ channels, including K_v4.2, tetramerize to form a single transmembrane pore (Birnbaum et al., 2004). These findings typified the results from three independent experiments. Co-expressed CD8 proteins tagged with myc and His at the C-terminus, displayed in the blot below (Fig. 4A), were used to check relative transfection efficiencies. The presence of these various multimers in our Western blots made quantification difficult. Instead, we performed protein dot blot assays to semiquantify the cell surface expression levels of K_v4.2 WT and mutant proteins. These semiquantification data are consistent with the Western blot analysis in showing that the surface expression levels of mutant proteins did not differ significantly from those of WT proteins (Fig. 4B).

Discussion

We describe here a *KCND2* truncation mutation that is, to our knowledge, the first account of a partial loss-of-function mutation in a potassium channel gene in TLE.

The c.2723_2727delAAACT mutation identified in this study causes a frame-shift resulting in a premature termination codon. mRNA containing this premature termination codon may be eliminated by nonsense-mediated mRNA decay (Hentze and Kulozik, 1999; Byers, 2002) and could lead to K_v4.2 channel haploinsufficiency. However, since this mutation occurs within the last exon, the mRNA containing this particular premature termination codon is likely to escape nonsense-mediated mRNA decay (Hentze and Kulozik, 1999; Byers, 2002) and is predicted to produce a truncated K_v4.2 channel protein, named K_v4.2-N587fsX1, lacking the last 44 amino acids in the carboxyl terminal.

The major finding of our electrophysiological analysis was reduced current density in cells harboring mutant K_v4.2-N587fsX1 channels. Our results mirror two previous reports of lowered current density in cells expressing laboratory-generated K_v4.2 channel constructs that carry missense or truncation mutations in their C-termini (Petrecca et al., 2000; Callsen et al., 2005). Taken together, the K_v4.2 C-terminus appears to be important for influencing whole-cell current amplitudes.

Whole-cell currents can be expressed by the equation $I=NiP_o$, where I is the macroscopic current, N is the total number of channels, i is the single channel conductance, and P_o is the channel open probability. N and i have fixed values, whereas P_o is a function of membrane potential and time. We estimated P_o differences

between wild-type and mutant channels by comparing the kinetics of activation, the steady-state inactivation, the inactivation time constant, and the recovery speed from the inactivated state. Because there were no significant differences in these parameters, it is possible that there are no P_o differences between wild-type and mutant channels. Nevertheless, since our surface protein biotinylation assays showed no significant differences in total surface expression between WT and mutant channels, smaller single channel conductance in mutant channels compared with that of WT channels could have led to the reduced current density in cells transfected with mutant proteins. Unfortunately, we were unable to obtain good single channel recordings and therefore cannot confirm the possibility of compromised channel conductance in K_v4.2-N587fsX1 mutant proteins.

The highly specialized subcellular compartmentalization of K_v4.2 within the soma and dendrites of neurons (Sheng et al., 1992), leading to unique distribution patterns in distinct cell types, with attendant differences in electrophysiological characteristics of the K_v4.2 channels, may be critical for modulating synaptic transmissions (Birnbaum et al., 2004). There is a growing number of identified proteins which mediate K_v4.2 intraneuronal distribution, including a specific kinesin isoform, Kif17, which was recently shown to be important for targeting K_v4.2 to dendrites via the extreme C-terminus of K_v4.2 (Chu et al., 2006). In heterologous systems, there appears to be a strong surface membrane clustering effect induced by K_v4.2 interactions with cytoskeletal elements, such as filamin (Petrecca et al., 2000) and PSD-95 (Wong et al., 2002), which may parallel the imputed roles played by these scaffolding proteins in determining K_v4.2 somatodendritic distribution patterns in hippocampal neurons. Interestingly, the region deleted in K_v4.2-N587fsX1 mutant proteins harbors interacting motifs for both these cytoskeletal proteins.

Other scaffolding proteins may also affect K_v4.2 channel electrophysiology. Actin cytoskeletal changes induced by cytochalasin D treatment potently increased whole-cell K_v4.2 currents and focal channel expression in HEK cells (Wang et al., 2004). Hence, the reduced current density observed in our heterologous assay system may involve compromised interactions between mutant K_v4.2 and critical scaffolding proteins. Any resulting lability could then possibly translate into lowered current density.

Within crucial neurons, the absence of filamin- and/or PSD-95-directed surface expression may propagate a more random trafficking of K_v4.2-N587fsX1 mutant proteins, thereby altering overall somatodendritic K_v4.2 expression sufficiently to reduce I_A. Consequently, alterations in the inhibitory I_A, effected via any of the above paradigms, could disrupt the delicate balance between excitation and inhibition in specific neurons and contribute to the aberrant neuronal excitability typifying TLE.

Mesial TLE (mTLE) is often cited as the most common type of human epilepsy and is almost invariably accompanied by hippocampal sclerosis (Engel, 2001), although hippocampal atrophy is not, perforce, directly related to manifest epileptic symptoms (Kobayashi et al., 2002). The proband harboring the K_v4.2-N587fsX1 mutation, while diagnosed with mTLE, has a phenotype distinct from that of most other patients in our sample pool in that no overt histopathologies were evident in her resected tissues. Nonetheless, the surgically remediable outcome, with the patient remaining seizure-free 3 years after left anterior temporal lobectomy, tellingly points to some underlying pathology, critical to epileptogenesis, inherent within the resected tissues. We examined surgically obtained brain tissue samples from the proband by immunohistochemistry using an anti-K_v4.2 antibody, but we could not obtain definitive results (data not shown) and cannot rule out the presence of some subtle neuronal lesion in this case. The putative seizure susceptibility arising from the K_v4.2-N587fsX1 mutation could have been modified and regulated by some environmental factor or lesion intrinsic and specific to the left temporal lobe, thereby restricting the pathology to this region. Such imparities are common in TLEs as spontaneous seizures usually arise from only one temporal lobe (Engel, 2001), and there are also some cases of inheritable asymmetric hippocampal atrophy (Fernandez et al., 1998).

TLE is believed to have a multifactorial etiology, with developmental, environmental, and genetic components (Engel, 2001). Crucially, the effects of any mutation are influenced by a multitude of environmental and genetic determinants and their impact can also be blunted by redundant systems or allelic imbalance. Incomplete penetrance has been reported in familial TLE (Kobayashi et al., 2002), and this may account for the finding of the K_v4.2-N587fsX1 mutation in the proband's non-symptomatic father. Similarly, allelic imbalance, whereby the expression levels of mutant versus normal mRNA are differentially regulated in phenotypically affected and unaffected individuals, has been described in at least one channelopathy (Duno et al., 2004) and may be operating here—such variable expressivity may have produced a clinically much less severe version of the phenotype in the father. Mosaicism is another possibility in this case, *viz.* the K_v4.2-N587fsX1 mutation in the father may be restricted to certain cell lineages. Although we found the same mutation in the father's buccal and hair samples, the question of mosaicism remains indeterminate as the proband's grandparents are deceased and we obviously cannot exclude mosaicism within critically relevant regions of the father's brain. Lastly, given the small pedigree size and inconsistent mutation-to-disease segregation, we cannot exclude the possibility that this K_v4.2-N587fsX1 mutation is simply coincident with but unrelated to the disease.

Although genetic polymorphisms in at least seven genes have previously been associated with TLE, a recent study of 339 European TLE patients failed to replicate any association between TLE and common variants of these genes (Cavalleri et al., 2005). Genetic etiological factors in the common TLEs probably involve multiple rare susceptibility genes working via non-Mendelian inheritance mechanisms (Vadlamudi et al., 2003). Our study suggests that *KCND2* may represent one such rare susceptibility gene for TLE, but this finding is preliminary and more comprehensive investigations involving larger patient pools will be needed to clarify the roles of K_v4.2 in epilepsy.

Acknowledgments

We thank all the patients and families for their contributions and cooperation; T. Suzuki for laboratory support; Dr. S. Hirose for providing materials; Dr. T. Hashikawa for use of his laboratory space and apparatuses; and the Research Resource Center of the RIKEN Brain Science Institute for DNA sequencing analyses.

References

Adams, J.P., Anderson, A.E., Varga, A.W., Dineley, K.T., Cook, R.G., Pfaffinger, P.J., Sweatt, J.D., 2000. The A-type potassium channel K_v4.2 is a substrate for the mitogen-activated protein kinase ERK. J. Neurochem. 75, 2277–2287.

Bagetta, G., Nistico, G., Dolly, J.O., 1992. Production of seizures and brain damage in rats by α-dendrotoxin, a selective K^+ channel blocker. Neurosci. Lett. 139, 34–40.

Barnwell, L., Xu, X., Lin, X., Lueng, V., Anderson, A., 2004. Increased Seizure Susceptibility in K_v4.2 Null Mice. Abstract Viewer/Itinerary Planner. Society for Neuroscience, Washington, DC.

Beck, H., Clusmann, H., Kral, T., Schramm, J., Heinemann, U., Elger, C.E., 1997. Potassium currents in acutely isolated human hippocampal dentate granule cells. J. Physiol. 498 (Pt 1), 73–85.

Bernard, C., Anderson, A., Becker, A., Poolos, N.P., Beck, H., Johnston, D., 2004. Acquired dendritic channelopathy in temporal lobe epilepsy. Science 305, 532–535.

Birnbaum, S.G., Varga, A.W., Yuan, L.L., Anderson, A.E., Sweatt, J.D., Schrader, L.A., 2004. Structure and function of K_v4.-family transient potassium channels. Physiol. Rev. 84, 803–833.

Byers, P.H., 2002. Killing the messenger: new insights into nonsense-mediated mRNA decay. J. Clin. Invest. 109, 3–6.

Callsen, B., Isbrandt, D., Sauter, K., Hartmann, L.S., Pongs, O., Bahring, R., 2005. Contribution of N- and C-terminal K_v4.2 channel domains to KChIP interaction. J. Physiol. 568, 397–412.

Castro, P.A., Cooper, E.C., Lowenstein, D.H., Baraban, S.C., 2001. Hippocampal heterotopia lack functional K_v4.2 potassium channels in the methylazoxymethanol model of cortical malformations and epilepsy. J. Neurosci. 21, 6626–6634.

Cavalleri, G.L., Lynch, J.M., Depondt, C., Burley, M.W., Wood, N.W., Sisodiya, S.M., Goldstein, D.B., 2005. Failure to replicate previously reported genetic associations with sporadic temporal lobe epilepsy: where to from here? Brain 128, 1832–1840.

Chu, P.J., Rivera, J.F., Arnold, D.B., 2006. A role for Kif17 in transport of K_v4.2. J. Biol. Chem. 281, 365–373.

Duno, M., Colding-Jorgensen, E., Grunnet, M., Jespersen, T., Vissing, J., Schwartz, M., 2004. Difference in allelic expression of the *CLCN1* gene and the possible influence on the myotonia congenita phenotype. Eur. J. Hum. Genet. 12, 738–743.

Engel Jr., J., 2001. Mesial temporal lobe epilepsy: what have we learned? Neuroscientist 7, 340–352.

Fernandez, G., Effenberger, O., Vinz, B., Steinlein, O., Elger, C.E., Dohring, W., Heinze, H.J., 1998. Hippocampal malformation as a cause of familial febrile convulsions and subsequent hippocampal sclerosis. Neurology 50, 909–917.

Hentze, M.W., Kulozik, A.E., 1999. A perfect message: RNA surveillance and nonsense-mediated decay. Cell 96, 307–310.

Hoffman, D.A., Magee, J.C., Colbert, C.M., Johnston, D., 1997. K^+ channel regulation of signal propagation in dendrites of hippocampal pyramidal neurons. Nature 387, 869–875.

Juhng, K.N., Kokate, T.G., Yamaguchi, S., Kim, B.Y., Rogowski, R.S., Blaustein, M.P., Rogawski, M.A., 1999. Induction of seizures by the potent K^+ channel-blocking scorpion venom peptide toxins tityustoxin-Kα and pandinustoxin-Kα. Epilepsy Res. 34, 177–186.

Kalachikov, S., Evgrafov, O., Ross, B., Winawer, M., Barker-Cummings, C., Martinelli Boneschi, F., Choi, C., Morozov, P., Das, K., Teplitskaya, E., Yu, A., Cayanis, E., Penchaszadeh, G., Kottmann, A.H., Pedley, T.A., Hauser, W.A., Ottman, R., Gilliam, T.C., 2002. Mutations in *LGI1* cause autosomal-dominant partial epilepsy with auditory features. Nat. Genet. 30, 335–341.

Kobayashi, E., Li, L.M., Lopes-Cendes, I., Cendes, F., 2002. Magnetic resonance imaging evidence of hippocampal sclerosis in asymptomatic, first-degree relatives of patients with familial mesial temporal lobe epilepsy. Arch. Neurol. 59, 1891–1894.

Petrecca, K., Miller, D.M., Shrier, A., 2000. Localization and enhanced current density of the K_v4.2 potassium channel by interaction with the actin-binding protein filamin. J. Neurosci. 20, 8736–8744.

Rüschenschmidt, C., Kohling, R., Schwarz, M., Straub, H., Gorji, A., Siep, E., Ebner, A., Pannek, H.W., Tuxhorn, I., Wolf, P., Speckmann, E.J., 2004. Characterization of a fast transient outward current in neocortical neurons from epilepsy patients. J. Neurosci. Res. 75, 807–816.

Sheng, M., Tsaur, M.L., Jan, Y.N., Jan, L.Y., 1992. Subcellular segregation of two A-type K^+ channel proteins in rat central neurons. Neuron 9, 271–284.

Tsaur, M.L., Sheng, M., Lowenstein, D.H., Jan, Y.N., Jan, L.Y., 1992. Differential expression of K^+ channel mRNAs in the rat brain and down-regulation in the hippocampus following seizures. Neuron 8, 1055–1067.

Vadlamudi, L., Scheffer, I.E., Berkovic, S.F., 2003. Genetics of temporal lobe epilepsy. J. Neurol. Neurosurg. Psychiatry 74, 1359–1361.

Wang, Z., Eldstrom, J.R., Jantzi, J., Moore, E.D., Fedida, D., 2004. Increased focal K_v4.2 channel expression at the plasma membrane is the result of actin depolymerization. Am. J. Physiol.: Heart Circ. Physiol. 286, H749–H759.

Wong, W., Newell, E.W., Jugloff, D.G., Jones, O.T., Schlichter, L.C., 2002. Cell surface targeting and clustering interactions between heterologously expressed PSD-95 and the Shal voltage-gated potassium channel, K_v4.2. J. Biol. Chem. 277, 20423–20430.

Yuan, L.L., Adams, J.P., Swank, M., Sweatt, J.D., Johnston, D., 2002. Protein kinase modulation of dendritic K^+ channels in hippocampus involves a mitogen-activated protein kinase pathway. J. Neurosci. 22, 4860–4868.